Absence of small-world effects at the quantum level and stability of the quantum critical point

Massimo Ostilli*
Instituto de Física, Universidade Federal da Bahia, Salvador 40170-115, Brazil

(Received 25 November 2019; accepted 31 October 2020; published 23 November 2020)

The small-world effect is a universal feature used to explain many different phenomena like percolation, diffusion, and consensus. Starting from any regular lattice of N sites, the small-world effect can be attained by rewiring randomly an $O(N)$ number of links or by superimposing an equivalent number of new links onto the system. In a classical system this procedure is known to change radically its critical point and behavior, the new system being always effectively mean-field. Here, we prove that at the quantum level the above scenario does not apply: when an $O(N)$ number of new couplings are randomly superimposed onto a quantum Ising chain, its quantum critical point and behavior both remain unchanged. In other words, at zero temperature quantum fluctuations destroy any small-world effect. This exact result sheds new light on the significance of the quantum critical point as a thermodynamically stable feature of nature that has no analogy at the classical level and essentially prevents a naive application of network theory to quantum systems. The derivation is obtained by combining the quantum-classical mapping with a simple topological argument.

DOI: 10.1103/PhysRevE.102.052126

I. INTRODUCTION

After Onsager' s exact solution for the $D = 2$-dimensional case [1], the Ising model assumed the role of a paradigm at the base of our understanding of phase transitions and critical phenomena, not only within classical physics but also within quantum physics. However, important conceptual and quantitative differences exist between the two cases. In the classical case, competition between order and thermal fluctuations induces a second-order phase transition triggered by lowering the temperature below a critical value which is finite if $D \geqslant 2$. In the quantum case, at zero temperature, the competition between two different ground states induces a second-order phase transition triggered by lowering a transverse external field below a critical value which is finite even when $D = 1$ [2–6]. Indeed, as the quantum-classical mapping (QCM) shows [7], the critical behavior of a D-dimensional quantum Ising model amounts to that of a suitable $D + 1$ classical Ising model. Despite these well established facts and an extensive literature on the subject, many issues remain open about the interplay between the classical and the quantum case [3].

Aside from the finite-dimensional case, the classical Ising model and its generalizations have extensively been used also in the context of networks (complex or not), where the nodes and the links of the network represent the spins and the couplings between them, respectively [8–17]. In these systems, the phase transition is seen as a result of the interplay between the topology of the underlying network, ranging from completely regular to completely random, and the physical process running on it. Whenever the topology is sufficiently random these complex systems share a common feature: their dimension is effectively infinite and, as a consequence, the system is effectively mean-field. This property can be understood by exploiting the small-world (SW) concept [10]. In fact, the general feature of random graphs and their variants, called SW graphs, is their SW character: as opposed to D-dimensional lattices, where the average distance between two randomly chosen nodes scales as $N^{1/D}$, in SW graphs the distance scales as $\log(N)$, from which, by comparison, we see that in the latter case $D = \infty$. In terms of phase transitions, this SW property results in dramatically favoring long-range order, the system being effectively mean-field due to the infinite dimensionality [17]. However, the above scenario applies to classical systems and a natural question emerges: Does it hold for quantum systems too? Indeed, a bunch of speculative works trying to exploit the SW effect as well as the general concepts of complex networks at the quantum level have appeared in recent years [18] in which, e.g., Anderson localization is reduced [19], entanglement is improved [20], super conductivity is enhanced [21], and even the way to a visionary quantum internet is paved [22], to mention a few. Our finding, however, which is based on an exact result at zero temperature, leads to skepticism.

Let us consider specifically the SW graphs: Starting from any regular D-dimensional lattice, the SW property can be attained by rewiring an $O(N)$ number of couplings or by superimposing an equivalent number of extra couplings onto the original system. The latter procedure generates more analytically treatable models and several exact results have been reached [23,24], also for the $D \geqslant 2$ case [25,26]. In particular, for the classical Ising model these studies show that, due to the SW effect, in the $D = 1$ case the system acquires a finite critical temperature, while in the $D = 2$ case the system gets a higher critical temperature, and, in both cases, the critical behavior turns out to be mean-field-like.

Here we prove that this classical scenario does not hold at the quantum level: when an $O(N)$ number of extra ferromagnetic couplings are randomly superimposed onto a $D = 1$

*massimo.ostilli@gmail.com

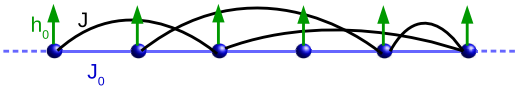

FIG. 1. A portion of the model studied in this paper: six qubits in a chain are immersed in a uniform transverse field h_0 (green arrows) and interact by nearest neighbors and random pairs via the ferromagnetic couplings J_0 (blue links) and J (black links), respectively. The mean connectivity related to the coupling J is denoted by c. When $h_0 \to 0$, we recover a classical Ising model whose underlying graph, despite being embedded in a one-dimensional space, is characterized by the SW effect and, as a consequence, makes the critical behavior of the classical model mean-field. However, does such a classical scenario hold also in the quantum case, i.e., when $h_0 \neq 0$?

quantum Ising chain (see Fig. 1), its quantum critical point and behavior both remain unchanged (see Fig. 2). In other words, at zero temperature quantum fluctuations destroy any SW effect. As we shall show, the ultimate reason for that is the fact that, at zero temperature, an extra dimension—the one associated with the imaginary time evolution—arises that is not covered by the SW links: the "quantum graph" is never SW. As a consequence, caution is in order before transferring the established knowledge of classical complex systems into the quantum world. This exact result sheds new light on the meaning of the quantum critical point as a thermodynamically stable feature of systems and, as we explain later, provides insights for understanding the intrigued interplay between quantum and classical behavior at finite temperatures in the presence of a transverse field [3]. Furthermore, the stability of the quantum critical point might be crucial for determining optimal quantum annealing paths [27–33] for hard

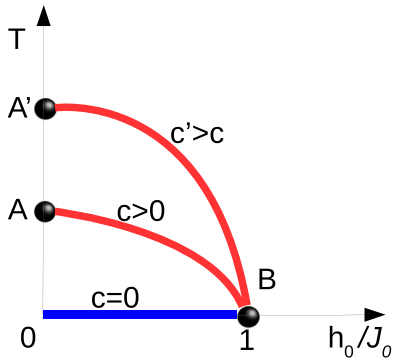

FIG. 2. Phase diagram of the quantum Ising chain of Fig. 1, Eq. (9), on the plane $(h_0/J_0, T)$, where J_0 is the coupling and h_0 is the transverse field. The curves $c > 0$ and $c' > c$ (red) represent qualitative lines of critical temperature for two different values of the additional mean connectivity (bringing the same long-range coupling J), c and c', as a function of the adimensional parameter h_0/J_0. For $c = 0$ the line of critical temperature collapses to 0 (blue). The points A (or A') and B represent classical and quantum critical points, respectively, and can be exactly calculated: $A \equiv [0, T_c(h_0 = 0)]$, $T_c(h_0 = 0)$ being the solution of Eq. (19), while $B \equiv (1, 0)$ for any c, this being the main result of the present work. The critical behavior in A (or A') is mean-field while that in B corresponds to that of a $D = 2$ Ising model. As we increase c toward c', the point A moves upward toward A', but B does not move at all.

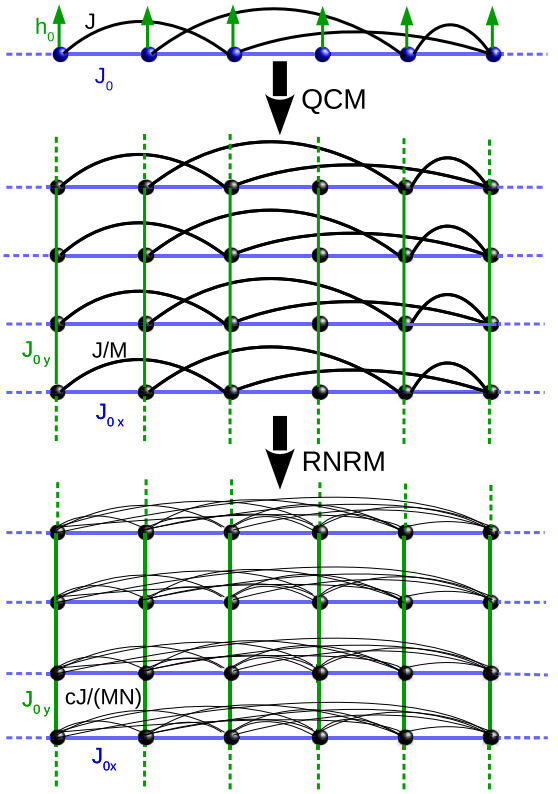

FIG. 3. Application of the quantum-classical mapping (QCM) followed by the random-nonrandom mapping (RNRM) to the quantum Ising chain of Eq. (9). Here $M = 4$ and $N = 6$. Dashed lines represent periodic boundary conditions. Top: Six qubits in a chain are immersed in a uniform transverse field h_0 (green arrows) and interact by nearest neighbors and random pairs via the ferromagnetic couplings J_0 (blue links) and J (black links), respectively. Notice that, in the classical limit, i.e., in the case with a null transverse field, $h_0 = 0$, the underlying network, even if embedded in a 1D space, makes the system SW. Middle: Array of 4×6 classical spins interacting by nearest neighbors via the couplings J_{0x} (blue links) and J_{0y} (green links), as given by Eqs. (3), and by random pairs via the coupling J/M (black links). Notice the absence of long-range links in the vertical direction, a fact that prevents the underlying network, now embedded in a 2D space, to make the system SW. Bottom: Array of 4×6 classical spins each interacting with nearest neighbors by the couplings J_{0x} and J_{0y}, and with all the other spins lying on the same row by the uniform coupling $cJ/(MN)$, as given by Eq. (11) for large M. This classical model can be exactly solved by using the exact solution of the 2D Ising model in the presence of a uniform external field (see Sec. V).

combinatorial problems [34–43]. The main aim of the present work however is to focus on the proof of the result. The first part of this result, i.e., the fact that there is no SW effect in a quantum system, is first made evident by using a quite simple geometrical argument based on the quantum-classical mapping (see top and middle panels of Fig. 3). Then, the second part of the result, i.e., the fact that the critical point remains unchanged when the random extra couplings are added, is derived by using another special mapping that sends a random model toward a nonrandom one (see bottom panel of Fig. 3). Furthermore, it is shown that this second mapping

confirms also that the critical behavior of the system remains unchanged: a fact that represents a necessary and sufficient condition for the absence of any SW effect and which is in agreement with the above simple geometrical argument.

The paper is organized as follows. In Sec. II we recall the QCM and its immediate application to the one-dimensional (1D) model without disorder (the pure model). In Sec. III we discuss the crucial difference of the QCM at zero and finite temperature (not often stressed in the literature). In Sec. IV we introduce the random model to which we apply the QCM followed by the application of the random-nonrandom mapping (RNRM), which eventually produces a model without disorder. In Sec. V we solve this model at $T = 0$. In Sec. VI we discuss the state of the art at $T > 0$. Finally, in Sec. VII conclusions are drawn. In the Appendix we report and revisit the derivation of the RNRM, originally given in Ref. [44], and provide also an alternative derivation.

II. THE PURE MODEL AND THE QCM

Let us consider a lattice ring of N qubits interacting via a first-neighbor ferromagnetic coupling, $J_0 > 0$, and subjected to a transverse field, h_0:

$$H_0 = -J_0 \sum_{i=1}^{N} \sigma_i^Z \sigma_{i+1}^Z - h_0 \sum_{i=1}^{N} \sigma_i^X, \tag{1}$$

where σ_i^X, σ_i^Y, and σ_i^Z are the Pauli matrices of the ith qubit. This system is known to develop a zero temperature second-order quantum phase transition at the critical point $J_0 = h_0$. A way to see this consists in solving the model via the Jordan-Wigner transformations [45,46]. Another interesting way consists in applying the QCM [7]. For $\beta \to \infty$, the QCM evaluates the partition function $Z_0 = \mathrm{Tr}\exp(-\beta H_0)$ of the quantum $D = 1$ model with Hamiltonian (1) as the partition function of an anisotropic classical $D = 2$ Ising model defined by two suitable couplings associated with two directions x and y (not to be confused with the suffix of the Pauli matrices): x corresponds to the position of the actual ith qbit, and y corresponds to a virtual direction along which we propagate the inverse temperature β (or, equivalently, the imaginary time). The resulting classical Hamiltonian reads (for a review see, e.g., Refs. [3,6])

$$\begin{aligned} H_0^{\mathrm{Classic}} = &- J_{0x} \sum_{j=1}^{M} \sum_{i=1}^{N} S_{i,j} S_{i+1,j} \\ &- J_{0y} \sum_{i=1}^{N} \sum_{j=1}^{M} S_{i,j} S_{i,j+1}, \end{aligned} \tag{2}$$

where the $S_{i,j}$ are MN virtual classical spins arranged onto the $D = 2$ discrete torus $[1,\ldots,M] \times [1,\ldots,N]$ and, up to terms $O(1/M^2)$, the two couplings are given as follows:

$$J_{0x} = \frac{J_0}{M}, \quad \beta_0 J_{0y} = \frac{1}{2} \ln\left(\frac{M}{\beta_0 h_0}\right), \tag{3}$$

where $\beta_0 = 1[\beta]$ is a unitary constant that serves only for dimensional reasons ($[\beta_0] = [\beta]$). Systems (1) and (2) become equivalent in the limit $M \to \infty$, i.e, in the limit in which the Trotter-Suzuki factorization [7], at the base of the QCM, becomes exact. In this limit, $J_{0x} \to 0^+$ while $J_{0y} \to +\infty$ in such a way that the system can have a finite critical point. In fact, by plugging Eqs. (3) into the equation for the critical point of the $D = 2$ Ising model (from Kramers-Wannier duality [47] or Onsager' s solution [1]),

$$\sinh(2\beta_0 J_{0x}) \sinh(2\beta_0 J_{0y}) = 1, \tag{4}$$

in the limit $M \to \infty$, we get the critical point of the original $D = 1$ quantum system (1): $J_0 = h_0$.

III. QCM AT ZERO AND FINITE TEMPERATURE—TECHNICAL WARNINGS

In the following sections, the reader should take into account two technical warnings not often stressed in the literature. These warnings are related to the crucial difference that exists between the application of QCM at zero and finite temperature.

(i) As first remarked by Suzuki [7], the QCM does not claim that the critical behavior of the D-dimensional quantum system H_0 at finite temperatures is equal to that of the $D+1$-dimensional classical system H_0^{Classic} since, for any finite β, the latter, due to Eqs. (3), degenerates when $M \to \infty$, so that, in general, at finite temperature, the resulting classical model might be equivalent to a suitable classical—but rather nonobvious—D-dimensional model. Let us analyze this issue more closely. It is easy to see that, in the thermodynamic limit, the ground-state energy E_0 of the system (1) can be expressed as

$$\begin{aligned} \lim_{N\to\infty} \frac{E_0}{N} &= -\lim_{N\to\infty} \lim_{\beta\to\infty} \frac{1}{N\beta} \log\left[\mathrm{Tr}\exp(-\beta H_0)\right] \\ &= -\frac{1}{\beta_0} \lim_{M,N\to\infty} \frac{1}{MN} \log\left[\mathrm{Tr}\exp\left(-\beta_0 H_0^{\mathrm{Classic}}\right)\right], \end{aligned} \tag{5}$$

where the last equality holds up to an immaterial additive constant that does not depend on the Hamiltonian parameters (see Sec. IV of Ref. [7]). From Eq. (5) it is then evident that, apart from the physical dimension, the length M plays the same role of the inverse temperature in the limit in which this goes to infinity and, as a consequence, the zero temperature limit is also the limit $M \to \infty$ where the Trotter-Suzuki factorization becomes exact. At finite temperature, one can still exactly exploit the Trotter-Suzuki factorization, but the resulting classical system does not acquire an actual extra dimension. In fact, at finite temperature one has to evaluate the free energy density f_0 as

$$\begin{aligned} -\beta f_0 &= \lim_{N\to\infty} \frac{1}{N} \log\left[\mathrm{Tr}\exp(-\beta H_0)\right] \\ &= \lim_{N\to\infty} \frac{1}{N} \log\left[\lim_{M\to\infty} Z_0^{\mathrm{Classic}}\right], \end{aligned} \tag{6}$$

which is very different from $\lim_{M,N\to\infty} \frac{1}{MN} \log[Z_0^{\mathrm{Classic}}]$. The finite temperature analysis is therefore rather harder because it requires the exact solution of the $D = 2$ model for finite sizes where one of the two sides of the torus must be sent to infinity while keeping the other fixed. In particular, as shown in Ref. [7], for the model (1) it is possible to obtain f_0 by

exploiting the exact solution of the $D = 2$ Ising model for finite sizes from Kaufman [48] and the result is

$$-\beta f_0 = \frac{1}{2\pi}\int_0^{2\pi} dq \log\left[2\cosh\left(\beta\epsilon(q)\right)\right], \tag{7}$$

where

$$\epsilon(q) = \left[J_0^2 + h_0^2 - 2J_0 h_0 \cos(q)\right]^{1/2}. \tag{8}$$

Remarkably, Eqs. (7) and (8) cannot be obtained from the thermodynamic limit of the free energy density of the $D = 2$ classical Ising model by simply using in it the couplings (3) in the limit $M \to \infty$. Notice in particular that, as anticipated, for any finite β, Eqs. (7) and (8) do not show any singularity in the Hamiltonian parameters or in β. Only for $\beta \to \infty$ does a singularity show up at the critical point $J_0 = h_0$ and only in this limit is one allowed to exploit the thermodynamic limit of the free energy density of the $D = 2$ classical Ising model by simply using in it the couplings (3) in the limit $M \to \infty$. Later on, we shall need to work with the free energy density of the $D = 2$ classical Ising model but in the presence of a row-dependent external field.

(ii) Provided the result is used only for zero temperature [see warning (i)], the QCM makes sense and is useful for analytic manipulations also for large but finite M, provided that M scales at least proportionally with N. As a practical rule one can simply take $M = N$.

We stress again that in the following analysis we are only concerned with the zero temperature limit and the symbol β_0 plays no role but a mere dimensional factor.

IV. THE MODEL WITH SMALL-WORLD COUPLINGS AND THE RNRM

Let us now see what happens when we add cN extra interactions between random pairs of qubits via another ferromagnetic coupling, $J > 0$, with $c > 0$ being the additional mean connectivity (see the upper panel of Fig. 3). The new quantum Hamiltonian reads

$$H = -J\sum_{i<j=1}^{N} c_{i,j}\sigma_i^Z\sigma_j^Z - J_0\sum_{i=1}^{N}\sigma_i^Z\sigma_{i+1}^Z - h_0\sum_{i=1}^{N}\sigma_i^X, \tag{9}$$

where $c_{i,j}$ is the adjacency matrix of the extra couplings, i.e., a random variable taking the values 0 or 1 with probabilities $1 - c/N$ or c/N, respectively. The resulting ensemble of graphs generated by the different realizations of $\{c_{i,j}\}$ is known as the Gilbert random graph (a slight variant of the Erdös-Reny random graph), and its properties are well known [11]. In particular, for large N, the connectivity of each node becomes poissonian distributed with mean c and, for any $c > 1$, the graph is percolating and owns the SW property. In general, for different realizations of $\{c_{i,j}\}$ there correspond different Hamiltonians (9). Yet, in the thermodynamic limit $N \to \infty$, due to the self-averaging character of the random graph, relative fluctuations of the system become negligible. In other words, any extensive observable (like the energy or the magnetization) can be evaluated either via a single realization of a sufficiently large system or as an average over the adjacency matrix realizations. The latter is the usual successful setup applied to all (quenched [8]) disordered models in classical physics which, thanks to the QCM, we can assume to be valid also in the present quantum case.

On applying the QCM to the quantum system (9) we get

$$H^{\text{Classic}} = -\frac{J}{M}\sum_{j=1}^{M}\sum_{i_1<i_2=1}^{N} c_{i_1,i_2}S_{i_1,j}S_{i_2,j} + H_0^{\text{Classic}}, \tag{10}$$

where H_0^{Classic} is defined in Eqs. (2) and (3). From the first term of Eq. (10), we see that the SW effect on the underlying graph of H^{Classic}, if any, can be realized only along the x direction (see the middle panel of Fig. 3). In other words, in order to cross the $D = 2$ torus $[1,\ldots,M]\times[1,\ldots,N]$ from one corner to the opposite via a sequence of random hoppings on the underlying graph of H^{Classic}, on average we must use an $O(\log(N)M)$ number of links, while in a SW graph this should be $O(\log(MN))$. As a consequence, we expect that H^{Classic}, and hence the quantum system governed by H, has not acquired a mean-field character and that it remains essentially similar to the original quantum system governed by H_0 with no SW effect. In the following we prove that this guess is exact in an extreme sense: not only the quantum critical behaviors but also the quantum critical points of H_0 and H are the same.

Let us indicate the averages over the $\{c_{i_1,i_2}\}$ realizations by $\overline{\cdot}$. As explained above, if $\langle O\rangle = \text{Tr}O\exp(-\beta H)/\text{Tr}\exp(-\beta H)$ denotes the ensemble average of the observable O associated with a given $\{c_{i_1,i_2}\}$ (quenched) realization, for large N we can conveniently identify this average with $\overline{\langle O\rangle}$. In turn, all these averages can essentially be derived from the free energy density f of the quenched model: $-\beta f = \lim_{N\to\infty}\overline{\ln(Z)}/N = \lim_{N\to\infty}\lim_{n\to 0}(\overline{Z^n} - 1)/(Nn)$. The latter identity is at the base of the so-called replica trick that has been used to investigate a large variety of random models, especially spin-glass models [8]. At the critical point, when the replica trick is used in combination with the high-temperature expansion of the free energy of a model built over a random graph, there emerges a general mapping between the random model (or "disordered model") and a suitable nonrandom model [25,44]. In the following, we refer to this mapping as the RNRM. In general, the disorder can be due to the underlying graph structure having a generic random matrix $\{c_{i_1,i_2}\}$ and, more in general, to the random values of the corresponding couplings $\{J_{i_1,i_2}\}$. In both cases, the RNRM consists of the following replacement (here $\overline{\cdot}$ means average over any kind of disorder)

$$c_{i_1,i_2}\tanh(\beta J_{i_1,i_2}) \to \overline{c_{i_1,i_2}\tanh\left(\beta J_{i_1,i_2}\right)}. \tag{11}$$

As has been confirmed also via Monte Carlo simulations [26], whereas the RNRM (11) gives only effective approximations below the critical temperature, it provides the exact critical point and behavior by ruling out all the difficulties of the random model. We stress that the RNRM does not consist of some annealed approximation. One of the most interesting advantages of the RNRM lies in the fact it holds true for generalized infinite-dimensional graphs without the necessity for such graphs to be locally treelike or small-world, just as in the present case. In the Appendix we report a simple derivation that is valid for the present case and show also an alternative derivation which does not invoke the replica trick at all. When applied to the adjacency matrix $\{c_{i_1,i_2}\}$ of the random graph with the constant coupling J/M, for large

but finite M, Eq. (11) sends the random classical Hamiltonian (10) to the following nonrandom Hamiltonian (see the bottom panel of Fig. 3):

$$\tilde{H}^{\text{Classic}} = -\frac{cJ}{MN}\sum_{j=1}^{M}\sum_{i_1<i_2=1}^{N} S_{i_1,j}S_{i_2,j} + H_0^{\text{Classic}}. \tag{12}$$

V. SOLUTION OF THE MODEL AT $T = 0$

The Hamiltonian $\tilde{H}^{\text{Classic}}$ represents a $D = 2$ Ising model with superimposed fully connected interactions that run only within the rows of the torus $[1, \ldots, M] \times [1, \ldots, N]$. Its partition function $\tilde{Z}^{\text{Classic}}$ of the model (12) can be analyzed by a standard technique [49]. By introducing M auxiliary-independent Gaussian fields $\{x_l\}$, up to a $O(1)$ term in the exponent, and up to an immaterial constant of proportionality, we get

$$\tilde{Z}^{\text{Classic}} \propto \int \prod_{j=1}^{M} dx_j e^{-N\beta_0 f(\{x_j\})}, \tag{13}$$

$$\beta_0 f(\{x_j\}) = \frac{c\beta_0 J}{M}\sum_{j=1}^{M} x_j^2 + \beta_0 f_0\left(\beta_0 J_{0x}, \beta_0 J_{0,y}; \left\{\frac{c\beta_0 J}{M} x_j\right\}\right), \tag{14}$$

where $f_0(\beta J_{0x}, \beta J_{0,y}; \{\beta h_j\})$ is the free energy density of the $D = 2$ Ising model with the couplings J_{0x} and J_{0y} in the presence of a row-dependent external field, $\{h_j\}$. Notice that, in order to avoid a pedant notation like $f_0(\beta J_{0x}, \beta J_{0,y}; \{\beta h_j\}; N, M)$, etc., in Eq. (13) and following, the harmless dependencies on finite-size effects are left understood but they should be kept in mind for the correct interpretation of the next equations. We stress that such dependencies on finite-size effects are smooth and not particularly important since, unlike the harder situation where one has to deal with finite temperatures [see warning (i)], here we have $N \sim M$. The steepest descent method applied to Eq. (13) provides the following effective mean-field equations for the row-dependent average magnetizations $m_j = \sum_{i=1}^{N}\langle S_{i,j}\rangle/N$ of Eq. (12):

$$m_j = m_{0;j}\left(\beta_0 J_{0x}, \beta_0 J_{0,y}; \left\{\frac{c\beta_0 J}{M} m_l\right\}\right), \quad j = 1, \ldots, M, \tag{15}$$

where $m_{0;j}(\beta_0 J_{0x}, \beta_0 J_{0,y}; \{\beta_0 h_j\})$ is the magnetization along the jth row of the $D = 2$ Ising model with the couplings J_{0x} and J_{0y} in the presence of a row-dependent external field, $\{h_j\}$. Equations (15) and following are valid up to $O(\log(N)/N)$ corrections. Let us focus on the thermodynamically dominant uniform solution $\{m_j = m\}$ [making $f(\{m_j\})$ a minimum]. By deriving Eq. (15) with respect to a uniform external field, $\{\beta h_j = \beta h\}$, we obtain the adimensional susceptibility of the system

$$\chi = \frac{\chi_0\left(\beta_0 J_{0x}, \beta_0 J_{0,y}; \frac{c\beta_0 J}{M} m\right)}{1 - \frac{c\beta_0 J}{M}\chi_0\left(\beta_0 J_{0x}, \beta_0 J_{0,y}; \frac{c\beta_0 J}{M} m\right)}, \tag{16}$$

where $\chi_0(\beta J_{0x}, \beta J_{0,y}; \beta h)$ is the adimensional susceptibility of the $D = 2$ Ising model with the couplings J_{0x} and J_{0y} in the presence of a uniform external field, h. The paramagnetic solution of Eq. (15) is stable when the denominator of Eq. (16) evaluated at $m = 0$ is positive. In other words, for finite M, the paramagnetic solution becomes unstable when

$$\frac{c\beta_0 J}{M}\chi_0(\beta_0 J_{0x}, \beta_0 J_{0,y}; 0) = 1. \tag{17}$$

Taking into account the critical point of the $D = 2$ model, Eq. (4), Eq. (17) tells us that, for large but finite M, the critical point of the system (12) is shifted at higher temperatures or, in terms of the couplings $\beta_0 J_{0x}$ and $\beta_0 J_{0,y}$, is such that $\sinh(2\beta_0 J_{0x})\sinh(2\beta_0 J_{0y}) < 1$. Furthermore, for large but finite M, Eq. (15) tells us that the system is essentially mean-field-like, with the classical critical exponents. In fact, from Eq. (16) we see that the susceptibility has the critical exponent $\gamma = 1$ and similarly for the other critical exponents. However, the QCM holds true only in the limit $M \to \infty$. In such a limit, Eq. (17) can be satisfied only at the critical point of the $D = 2$ model (4) [where $\chi_0(\beta_0 J_{0x}, \beta_0 J_{0,y}; 0) \to \infty$], which, by using explicitly the expression for the couplings, Eqs. (3), implies that the critical point of the quantum system with extra random couplings, Eq. (9), is just equal to the critical point of the quantum system without random couplings, Eq. (1): $J_0 = h_0$. Furthermore, if we choose $J_0 < h_0$, so that we are in the paramagnetic region, on sending $M \to \infty$ in Eq. (16), we get

$$\lim_{M\to\infty}\chi = \lim_{M\to\infty}\chi_0(\beta_0 J_{0x}, \beta_0 J_{0,y}; 0), \tag{18}$$

which implies that the critical exponent of the susceptibility of the system (9) is equal to the critical exponent of the susceptibility of the quantum system (1) ($\gamma = 7/4$), and the same argument applies to the other critical exponents. Notice that our analysis does not necessarily imply that the systems (1) and (9) at $T = 0$ are identical. As we have mentioned before, inside the ferromagnetic region, i.e., for $J_0 > h_0$, the RNRM is only an approximation where Eq. (15) turns out to be effective [26].

VI. STATE OF THE ART AT $T > 0$

The above result is limited to zero temperature. The other available exact result concerns the pure classical model, i.e., the case with no transverse field, $h_0 = 0$. As discussed in the introduction, in this case, for any $c > 0$ the system is effectively mean-field and its critical point can be exactly calculated by the following equation [24,25]:

$$c\tanh(\beta J)e^{2\beta J_0} = 1. \tag{19}$$

Equation (19) tells us that the critical temperature is a growing function of c (linear for large c). For any other case, i.e., the region ($h_0 > 0$, $T > 0$), there are no exact results; however, as discussed before in warning (i), in this region the $D = 1$ quantum system (1) behaves essentially as a $D = 1$ classical system (7), so that, analogously, we expect that for any $T > 0$ the $D = 1$ quantum system with superimposed additional links, Eq. (9), behaves essentially as a $D = 1$ classical system with superimposed additional links too, having therefore the small-world character, a finite critical temperature, and mean-field critical exponents. By using these observations and interpolating the exact points given by Eq. (19) and the

quantum critical point, we get the scenario depicted in Fig. 2, with a line of critical temperatures that grows with c for any $h_0 < J_0$.

For $T > 0$ the critical behavior is classical for any value of the Hamiltonian parameters; however, this does not imply that all the physics of the system is dominated by a classical behavior. More precisely, sufficiently far from the critical line, things might be not classical even for $T > 0$. In fact, when $c = 0$, for $T > 0$ two lines of a $D = 1$-classical $\rightarrow$ $D = 1$-quantum crossover are known to exist that depart from the quantum critical point $h_0 = J_0$ (for fixed T, the above crossing corresponds to transiting from $h_0 < J_0$ to $h_0 > j_0$) [2–4,6]. From the experimental point of view, this crossover region represents the most important part of the problem [3]. Our analysis leads one to expect that, for $c > 0$, such a crossover might become mean-field-classical $\rightarrow$ $D = 1$-quantum. This is a rather interesting issue that deserves further investigation.

VII. CONCLUSIONS AND PERSPECTIVES

In conclusion, we have proved that, contrary to a somehow classical common sense, at zero temperature there is no SW effect, the quantum critical point and behavior of the system remaining those of the finite-dimensional model before the addition of the extra links or, equivalently, before the rewiring. Quantum fluctuations destroy any SW effect and raise the quantum critical point as a robust feature of nature. Whereas this invariance puts severe limits on the possibility for improving long-range order via the SW effect at low temperatures, we expect possible applications for quantum annealing.

It is natural to ask whether the stability of the quantum critical point remains valid also for more general networks, in particular, those that are scale free. This will be the subject of a future work. It is should be, however, clear from our discussion based on the QCM (the same argument applies unchanged) that the small-world property cannot be satisfied regardless of the structure of the underlying network defined by the set of couplings, a general feature that prevents a naive application of network theory to quantum systems.

Our result is obtained by combining the quantum-classical mapping with a random-nonrandom mapping, the latter being based on a simple topological argument.

Note added. Recently, I became aware of an interesting work that by simulation shows the absence of the small-world effect in a photonic quantum network [50].

ACKNOWLEDGMENTS

Grant No. CNPq 307622/2018-5 is acknowledged. We thank T. Macrì and C. Presilla for a critical reading of the manuscript.

APPENDIX: RNRM

The RNRM was originally developed for analyzing spin-glass models, but in the case of ferromagnetic models its derivation is simpler, and it is worth reporting it here where we check its validation for the model with the Hamiltonian given by Eq. (10). For more details we refer the reader to Refs. [25,44]. We report also a different derivation not based on the replica trick. Let us consider an Ising model with N spins and generic couplings J_b along the bonds $b \equiv (i_b, j_b)$ of an undirected graph G whose set of links is denoted by Γ. The Hamiltonian and the partition function of this system read as follows:

$$H = -\sum_{b\in\Gamma} J_b \sigma_{i_b}\sigma_{j_b}, \tag{A1}$$

$$Z = \prod_b \cosh(\beta J_b) P, \tag{A2}$$

$$P = \sum_{\gamma\in\mathcal{G}} \prod_{b\in\gamma} t_b, \quad t_b \equiv \tanh(\beta J_b), \tag{A3}$$

where in Eqs. (A2) and (A3) we have applied the so-called high-temperature expansion, $\mathcal{G}$ being the set of (closed) multipolygons γ in G. From Eq. (A2) we see that in the thermodynamic limit the density free energy f splits as

$$-\beta f = \lim_{N\to\infty} \frac{1}{N} \sum_{b\in\Gamma} \log\left[\cosh(\beta J_b)\right] + \varphi, \tag{A4}$$

where

$$\varphi = \lim_{N\to\infty} \frac{\log(P)}{N}. \tag{A5}$$

Clearly, a singular behavior of f, if any, can be contained only in φ. Let us consider now that some disorder is present, in the graph G, in the couplings, or in both, and let us indicate by $\overline{\cdot}$ the average over this disorder. In other words, the factors t_b, with $b \in \Gamma$, must be seen as a set of independent random variables (not necessarily identically distributed). In such a case we are interested in evaluating

$$\overline{\varphi} = \lim_{N\to\infty} \frac{\overline{\log(P)}}{N} = \lim_{N\to\infty} \lim_{n\to 0} \frac{\overline{P^n} - 1}{Nn}. \tag{A6}$$

The replica trick consists in evaluating $\overline{P^n}$ for n integer and attempt the analytic continuation toward $n \to 0$. From Eq. (A3) we have

$$\overline{P^n} = \sum_{\gamma_1,\ldots,\gamma_n\in\overline{\mathcal{G}}} \prod_{b_1\in\gamma_1,\ldots,b_n\in\gamma_n} \overline{t_{b_1}\cdots t_{b_n}}, \tag{A7}$$

where $\overline{\mathcal{G}}$ is the natural extension of $\mathcal{G}$ that includes disorder, i.e., the set of multipolygons made by bonds $b \in \overline{\Gamma}$, where

$$\overline{\Gamma} = \{b = (i_b, j_b) : \overline{t_b} \neq 0\}. \tag{A8}$$

Let us analyze the first terms. We have

$$\overline{P^1} = \overline{P} = \sum_{\gamma\in\overline{\mathcal{G}}} \prod_{b\in\gamma} \overline{t_b}, \tag{A9}$$

$$\overline{P^2} = \sum_{\gamma_1,\gamma_2\in\overline{\mathcal{G}}} \prod_{b_1\in\gamma_1, b_2\in\gamma_2 : b_1\neq b_2} \overline{t_{b_1}}\cdot\overline{t_{b_2}} \prod_{b\in\gamma_1\cap\gamma_2} \overline{t_b^2}, \tag{A10}$$

$$\begin{aligned}\overline{P^3} = &\sum_{\gamma_1,\gamma_2,\gamma_3\in\overline{\mathcal{G}}} \prod_{b_1\in\gamma_1,b_2\in\gamma_2,b_3\in\gamma_3 : b_1\neq b_2, b_1\neq b_3, b_2\neq b_3} \overline{t_{b_1}}\cdot\overline{t_{b_2}}\cdot\overline{t_{b_3}} \\ &\times \prod_{b\in\gamma_1\cap\gamma_2, b'\in\gamma_3 : b\neq b'} \overline{t_b^2}\cdot\overline{t_{b'}} \prod_{b\in\gamma_1\cap\gamma_3, b'\in\gamma_2 : b\neq b'} \overline{t_b^2}\cdot\overline{t_{b'}} \\ &\times \prod_{b\in\gamma_2\cap\gamma_3, b'\in\gamma_1 : b\neq b'} \overline{t_b^2}\cdot\overline{t_{b'}} \prod_{b\in\gamma_1\cap\gamma_2\cap\gamma_3} \overline{t_b^3}.\end{aligned} \tag{A11}$$

Let us consider a disorder such that $\overline{t_b} \geqslant 0$. Depending on the kind of disorder, $\overline{\Gamma}$ can be "small" or "large." For example, if the disorder involves only the couplings of a lattice model with a fixed set of bonds Γ, we have $\overline{\Gamma} = \Gamma$ and the evaluation of $\overline{P^n}$ may remain very hard for $n \neq 1$, unless G is locally treelike, for which we have

$$\overline{P^n} \simeq \overline{P}^n. \tag{A12}$$

If instead the disorder is such that at any lattice point there pass a number N^α of bonds for some $\alpha > 0$, a simple combinatorial argument emerges: given two randomly chosen multipolygons γ_1 and γ_2 in $\overline{\mathcal{G}}$, the probability that they overlap along some bonds becomes negligible in the limit of large N. Notice that, due to the factors $\overline{t_b^k}$ in $\overline{P^n}$, with $k \in \{1, \ldots, n\}$, at high temperature and in the thermodynamic limit, $\overline{P^n}$ is characterized by only short multipolygons whose overlap, therefore, tends trivially to zero (simply because they are mostly disconnected). As we decrease the temperature, however, multipolygons of larger and larger length become important in $\overline{P^n}$. In fact, for a system characterized by a single coupling value and without disorder, i.e., a single value $t_b = \tanh(\beta J)$, φ is a power series in $\tanh(\beta J)$ as follows:

$$\varphi = \sum_{l=0}^{\infty} c_l \tanh^l(\beta J), \tag{A13}$$

where the coefficients c_l take into account the number of multipolygons of length l (see later for the actual connection between the c_l's and the numbers C_l's of multipolygons of length l) and therefore grow exponentially with l. As a consequence, the series has a radius of convergence R determined by the inverse of the ratio of growth of c_l, $R^{-1} = \lim_{l\to\infty} c_{l+1}/c_l$. The radius of convergence determines therefore the critical temperature of the system via the universal equation

$$\frac{1}{\tanh(\beta_c J)} = \lim_{l\to\infty} \frac{c_{l+1}}{c_l}. \tag{A14}$$

An analogous formula holds true also for the random system. Equation (A14) tells us that, at the critical point, the relevant information concerns only multipolygons of infinite length (later on, we comment about how the value of $\overline{\varphi}$ at the critical point characterizes its value in all the paramagnetic regions). This observation applies in particular to the evaluation of $\overline{P^2}$ via the analysis of two randomly chosen paths of infinite length. Whereas it is difficult to evaluate the probability that they overlap in general, it is easy to see that it goes to zero in many cases of interest by just looking at the possible paths that emanate from the same vertex. This combinatorial argument allows one to effectively neglect all the terms involving overlaps of bonds in Eqs. (A9)–(A11), which leads again to Eq. (A12), where the approximation becomes exact in the limit $N \to \infty$, regardless of the presence of short loops and regardless of the value of α. Notice that only for $\alpha = 1$ one has the small-world property.

More precisely the mechanism goes as follows. To fix the idea, let us consider an Ising model with the coupling J built over the Gilbert random graph, i.e., the graph where the adjacency matrix $c_{i,j}$ is a random variable taking value 0 or 1 with probabilities $1 - c/N$ or c/N, respectively. In this case we have $\overline{t_b^k} = \overline{t^k} = (c/N)\overline{\tanh^k(\beta J)}$. As we have explained in Sec. IV, in the thermodynamic limit, we are free to evaluate $\overline{f}$ and $\overline{\varphi}$ by either performing the average over all the graph realizations or considering a single but infinite graph (in other words the free energy is self-averaging). We apply the latter if $c < 1$ and the former if $c > 1$. If $c < 1$ we use the known fact that, in the thermodynamic limit, the Gilbert random graph has zero clustering coefficients. As a consequence, for $c < 1$ in the thermodynamic limit, loops are negligible and we have trivially $\overline{\varphi} = \varphi = 0$. Let us now consider the case $c > 1$ and let us evaluate $\overline{P^2}$. From Eq. (A10) we see that we have a sum over pairs of multipolygons which can have a zero, a full, or a partial overlap between each other. We can split the sum over all the pairs of multipolygons γ_1 and γ_2 of lengths l_1 and l_2, respectively, as follows:

$$\overline{P^2} = \sum_{l_1,l_2} [\mathcal{N}_0(l_1, l_2)(\overline{t})^{l_1+l_2} + \mathcal{N}_2(l_1, l_2)(\overline{t^2})^{(l_1+l_2)/2} + \cdots], \tag{A15}$$

where $\mathcal{N}_0(l_1, l_2)$ is the number of pairs of multipolygons which have zero overlap, $\mathcal{N}_2(l_1, l_2)$ is the number of pairs of multipolygons which have full overlap, and the dots stands for the rest of the contributions characterized by a partial overlap. To make more manifest the first two kinds of contributions, we find it convenient to rewrite the sum as

$$\overline{P^2} = \sum_{l=0}^{\infty} \left\{ \mathcal{N}_0(l) \left[\frac{c}{N} \tanh(\beta J) \right]^l + \mathcal{N}_2(l) \left[\frac{c}{N} \tanh^2(\beta J) \right]^{\frac{l}{2}} + \ldots \right\}, \tag{A16}$$

where $\mathcal{N}_0(l)$ is the total number of multipolygons of length l which can be formed by any pair of multipolygons having zero overlap, $\mathcal{N}_2(l)$ is the total number multipolygons formed by pairs of multipolygons each having length $l/2$ (for l even; clearly, for l odd we have $\mathcal{N}_2(l) = 0$), and we have made explicit use of $\overline{t^k} = (c/N)\overline{\tanh^k(\beta J)}$. Notice that here $\overline{\Gamma}$ corresponds to the complete (or fully connected) graph. Taking into account that in the complete graph of N nodes the number of paths of length l is N^l, we have $\mathcal{N}_0(l) \simeq [l(l+1)/2]N^l$ and $\mathcal{N}_2(l) = N^{l/2}$. In fact, we can form a global path of length l by combining two nonoverlapping paths having lengths l_1 and $l - l_1$, respectively, and there are $l(l+1)/2$ such combinations, whereas we can overlap a pair of paths only if they have the same length. In conclusion, the ratio between the second and the first kind of contribution is $1/(c^{l/2}l^2)$. Similar considerations hold true for the terms with a partial overlap. Taking into account now that $c > 1$, we see that, in the thermodynamic limit, for $l \to \infty$ Eq. (A16) can be evaluated by dropping all the terms except those associated with $\mathcal{N}_0(l)$.

By plugging Eq. (A12) in Eq. (A6) and by using Eq. (A9) we finally arrive at

$$\overline{\varphi} = \varphi_I(\{\overline{t_b}\}), \tag{A17}$$

which tells us that, up to an additive constant, the density free energy f of the random system is equal to the density free energy f_I of an Ising model whose set of nonrandom

couplings $\{J_b^{(I)}\}$ satisfies

$$\tanh\left(\beta J_b^{(I)}\right) = \overline{\tanh(\beta J_b)}. \tag{A18}$$

In particular, for the case of the generalized Gilbert random graph with fixed amplitudes related to the Hamiltonian (10), we see that the topological argument holds true for large N, so that in this case we have $\alpha = 1/2$ [the total number of nodes is MN with $M \sim N$, see warning (ii)] and Eq. (A18) amounts to [here (i_1, j_1) and (i_2, j_2) represent the positions of the two nodes between which there is the bond b, $J_b^{(I)} \equiv J^{(I)}_{(i_1,j_1;i_2,j_2)}$]

$$\tanh(\beta J^{(I)}_{(i_1,j_1;i_2,j_2)}) = \begin{cases} \frac{c}{N}\tanh\left(\beta J_{0x} + \frac{\beta J}{M}\right) + \left(1 - \frac{c}{N}\right)\tanh(\beta J_{0x}), & i_2 = i_1 + 1,\ j_2 = j_1, \\ \tanh(\beta J_{0y}), & j_2 = j_1 + 1,\ i_2 = i_1, \\ \frac{c}{N}\tanh\left(\frac{\beta J}{M}\right), & i_2 \neq i_1 + 1,\ j_2 = j_1, \end{cases} \tag{A19}$$

which for large M leads to the Ising nonrandom Hamiltonian (12).

It is instructive to derive the RNRM in another way which does not make use of the replica trick. For pedagogical reasons, let us first assume that $\mathcal{G}$ is the square lattice. In $\mathcal{G}$, the allowed multipolygons γ have lengths $l = 0, 4, 6, 8, \ldots$ Let us decompose P in Eq. (A3) (i.e., the singular part of the partition function) as

$$P = 1 + Q_4 + Q_6 + Q_8 + \ldots, \tag{A20}$$

where we have introduced the sums restricted to multipolygons of fixed length:

$$Q_l = \sum_{\substack{\gamma \in \mathcal{G}\,:\, b\in\gamma \\ l(\gamma) = l}} \prod_{b\in\gamma} t_b, \tag{A21}$$

$l(\gamma)$ being the length of the multipolygon γ. We have

$$\log(P) = Q_4 + Q_6 + Q_8 - \tfrac{1}{2}\left(Q_4^2 + Q_6^2 + Q_8^2 + \cdots\right) - (Q_4Q_6 + Q_4Q_8 + Q_6Q_8 + \cdots) + \cdots, \tag{A22}$$

which leads to

$$\log(P) = Q_4^{(c)} + Q_6^{(c)} + Q_8^{(c)} + \cdots, \tag{A23}$$

where $Q_l^{(c)}$ stands for the sum restricted to connected multipolygons of fixed length l, a connected multipolygon being a multipolygon that cannot be obtained by the product of two or more (disconnected) multipolygons (in fact, we could call them just "polygons"). The first few terms are

$$Q_4^{(c)} = Q_4, \tag{A24}$$

$$Q_6^{(c)} = Q_6, \tag{A25}$$

$$Q_8^{(c)} = Q_8 - \tfrac{1}{2}Q_4^2, \quad \ldots \tag{A26}$$

Notice that, whereas Q_l does not allow for overlaps of links, $Q_l^{(c)}$ in general does. For example, the case $l = 8$ in Eq. (A26) shows that, in $Q_8^{(c)}$, the contributions due to the product of two disconnected squares coming from the second term cancel out with the first term. However, not all the contributions coming from the second term cancel out with some of the first. In fact, such extra contributions are all those in which a partial or total overlap between two squares is present. Note that the most important feature of the $Q_l^{(c)}$'s is that they are extensive in the system size N, as it must be according to Eq. (A5). Indeed, in this framework we understand the previously mentioned connection between the coefficients c_l introduced in Eq. (A13) and the total number of multipolygons of length l, C_l: for a system characterized by a single coupling the relation between the c_l's and the C_l's is the same as the relation between the $Q_l^{(c)}$'s and the Q_l's. Let us now suppose that the couplings in Eq. (A1) are independent identically distributed random variables. From Eqs. (A23) and (A24)–(A26) we have

$$\overline{\log(P)} = \overline{Q_4^{(c)}} + \overline{Q_6^{(c)}} + \overline{Q_8^{(c)}} + \cdots, \tag{A27}$$

where

$$\overline{Q_4^{(c)}} = \overline{Q_4}, \tag{A28}$$

$$\overline{Q_6^{(c)}} = \overline{Q_6}, \tag{A29}$$

$$\overline{Q_8^{(c)}} = \overline{Q_8} - \tfrac{1}{2}\overline{Q_4^2}, \quad \ldots \tag{A30}$$

Of course $\overline{Q_4^2} \neq (\overline{Q_4})^2$, and similarly for higher-order terms. However, we recognize that the approximation $\overline{Q_4^2} \simeq (\overline{Q_4})^2$ becomes more and more accurate as we consider, instead of the two-dimensional lattice, a hypercube D-dimensional lattice with larger and larger values of D [for the same topological argument that we have previously applied in deriving Eq. (A12)]. We stress again that, both before and after averaging over the disorder, in Q_4^2 there are contributions that do not cancel out with some of those of Q_8 and that the former are those in which at least an overlap of two links is present. As we consider larger and larger values of D, such surviving contributions from $\overline{Q_4^2}$ become dominated by those pairs of squares where only a pair of links overlap with each other (more precisely, by neglecting the contribution with the full overlap with respect to the contributions with a single overlap, we make an error order, $1/D$). Now, this does not imply yet that, in evaluating $\overline{Q_8^{(c)}}$ for large D, $\overline{Q_4^2}$ and $(\overline{Q_4})^2$ can be taken as approximately equal, because of the presence of the above overlapping link which is associated with a term that does not cancel out with $\overline{Q_8}$. However, as we have discussed before, in the thermodynamic limit the leading contributions that characterize the critical behavior of the system are those associated with arbitrarily long multipolygons, i.e., $l \to \infty$, where a single link overlap does not play any

role. And the above argument can be repeated for any products of say k terms, $Q_{l_1}Q_{l_2}\dots Q_{l_k}$. This shows that, effectively, when $D\to\infty$ or, more in general, when $\overline{\mathcal{G}}$ [see definition (A8)] is such that any vertex has a number of neighbors which is an increasing function of N (as in our target model), we can take effectively $\overline{Q_{l_1}Q_{l_2}\dots Q_{l_k}} \simeq \overline{Q_{l_1}}\cdot\overline{Q_{l_2}}\cdots\overline{Q_{l_k}}$, which, by plugging in Eqs. (A28)–(A30) implies

$$\overline{Q_l^{(c)}} \simeq Q_l^{(c)}(\{\overline{t_b}\}), \tag{A31}$$

where $Q_l^{(c)}(\{\overline{t_b}\})$ stands for the contribution of the connected multipolygons of length l of a nonrandom system in which the random couplings $\{t_b\}$ are replaced by their averages over the disorder $\{\overline{t_b}\}$ and the approximation becomes exact in the thermodynamic limit. Equation (A31) leads immediately to Eq. (A17). This alternative derivation, despite being a little more complicated, shows that actually the RNRM can be proved without invoking any replica trick.

Above, we have proved the RNRM at the critical point, which is enough for the present paper. We point out, however, that the same mapping applies to all the paramagnetic region P. For example, by extending the RNRM to arbitrary disorder, including spin-glass disorder, it is possible to find the generalization of the Nishimori line [51] and, by analytic continuation, to show that $\overline{\varphi}$ takes the same value in all the P region. In particular, for a system with a fixed coupling built on the Gilbert random graph, this implies that $\overline{\varphi}\equiv 0$ in all the P region [52].

[1] L. Onsager, Phys. Rev. **65**, 117 (1944).
[2] S. L. Sondhi, S. M. Girvin, J. P. Carini, and D. Shahar, Rev. Mod. Phys. **69**, 315 (1997).
[3] S. Sachdev, *Quantum Phase Transitions* (Cambridge University, Cambridge, England, 1999).
[4] T. Vojta, Quantum Phase Transitions, in *Computational Statistical Physics* (Springer, Berlin, 2002).
[5] F. H. L. Essler, H. Frahm, F. Göhmann, A. Klümper, and V. E. Korepin, *The One-Dimensional Hubbard Model* (Cambridge University, Cambridge, England, 2005).
[6] A. Dutta *et al.*, *Quantum Phase Transitions in Transverse Field Spin Models: From Statistical Physics to Quantum Information* (Cambridge University, Cambridge, England, 2015).
[7] M. Suzuki, Prog. Theor. Phys. **56**, 1454 (1976).
[8] M. Mezard, G. Parisi, and M. A. Virasoro, *Spin Glass Theory and Beyond* (World Scientific, Singapore, 1987).
[9] K. H. Fischer and J. A. Hertz, *Spin Glasses* (Cambridge University, Cambridge, England, 1991).
[10] D. J. Watts and S. H. Strogatz, Nature (London) **393**, 440 (1998).
[11] B. Bollobás, *Random Graphs*, 2nd ed. (Cambridge University, Cambridge, England, 2001).
[12] O. C. Martin, R. Monasson, and R. Zecchina, Theor. Comput. Sci. **265**, 3 (2001).
[13] R. Albert and A. L. Barabási, Rev. Mod. Phys. **74**, 47 (2002).
[14] S. N. Dorogovtsev and J. F. F. Mendes, *Evolution of Networks* (Oxford University, Oxford, 2003).
[15] M. Newman, A. L. Barabási, and D. J. Watts, *The Structure and Dynamics of Networks*, Princeton Studies in Complexity Vol. 23 (Princeton University, Princeton, NJ, 2006).
[16] G. Caldarelli, *Scale-Free Networks*, Oxford Finance Series, (Oxford University, Oxford, 2007).
[17] S. N. Dorogovtsev, A. V. Goltsev, and J. F. F. Mendes, Rev. Mod. Phys. **80**, 1275 (2008).
[18] J. Biamonte, M. Faccin, and M. De Domenico, Commun. Phys. **2**, 53 (2019).
[19] C. P. Zhu and S.-J. Xiong, Phys. Rev. B **62**, 14780 (2000); M. Sade, T. Kalisky, S. Havlin, and R. Berkovits, Phys. Rev. E **72**, 066123 (2005); L. Jahnke, J. W. Kantelhardt, R. Berkovits, and S. Havlin, Phys. Rev. Lett. **101**, 175702 (2008).
[20] M. Cuquet and J. Calsamiglia, Phys. Rev. Lett. **103**, 240503 (2009); S. Perseguers, M. Lewenstein, A. Acín, and J. I. Cirac, Nat. Phys. **6**, 539 (2010).
[21] G. Bianconi, Phys. Rev. E **85**, 061113 (2012).
[22] S. Wehner, D. Elkouss, and R. Hanson, Science **362**, 303 (2018).
[23] M. B. Hastings, Phys. Rev. Lett. **91**, 098701 (2003).
[24] T. Nikoletopoulos *et al.*, J. Phys. A: Math. Gen. **37**, 6455 (2004).
[25] M. Ostilli and J. F. F. Mendes, Phys. Rev. E **78**, 031102 (2008).
[26] A. L. Ferreira, J. F. F. Mendes, and M. Ostilli, Phys. Rev. E **82**, 011141 (2010).
[27] T. Kadowaki and H. Nishimori, Phys. Rev. E **58**, 5355 (1998).
[28] E. Farhi, J. Goldstone, S. Gutmann, and M. Sipser, arXiv:quant-ph/0001106.
[29] E. Farhi, J. Goldstone, S. Gutmann, J. Lapan, A. Lundgren, and D. Preda, Science **292**, 472 (2001).
[30] G. E. Santoro and E. Tosatti, J. Phys. A: Math. Gen. **39**, R393 (2006).
[31] S. Morita and H. Nishimori, J. Math. Phys. **49**, 125210 (2008).
[32] A. Das and B. K. Chakrabarti, Rev. Mod. Phys. **80**, 1061 (2008).
[33] T. Albash and D. A. Lidar, Rev. Mod. Phys. **90**, 015002 (2018).
[34] D. A. Battaglia, G. E. Santoro, and E. Tosatti, Phys. Rev. E **71**, 066707 (2005).
[35] T. Jörg, F. Krzakala, J. Kurchan, and A. C. Maggs, Phys. Rev. Lett. **101**, 147204 (2008).
[36] T. Jög, F. Krzakala, J. Kurchan, A. C. Maggs, and J. Pujos, Europhys. Lett. **89**, 40004 (2010).
[37] I. Hen, J. Job, T. Albash, T. F. Rønnow, M. Troyer, and D. A. Lidar, Phys. Rev. A **92**, 042325 (2015).
[38] V. S. Denchev, S. Boixo, S. V. Isakov, N. Ding, R. Babbush, V. Smelyanskiy, J. Martinis, and H. Neven, Phys. Rev. X **6**, 031015 (2016).
[39] S. Mandrà, G. G. Guerreschi, and A. Aspuru-Guzik, New J. Phys. **18**, 073003 (2016).
[40] S. Mandrà and H. G. Katzgraber, Quantum Sci. Technol. **3**, 04LT01 (2018).
[41] S. Mandrà and H. G. Katzgraber, Quantum Sci. Technol. **2**, 038501 (2017).
[42] H. G. Katzgraber and M. A. Novotny, Phys. Rev. Appl. **10**, 054004 (2018).
[43] C. Presilla and M. Ostilli, Phys. A (Amsterdam, Neth.) **515**, 57 (2019).

[44] M. Ostilli, J. Stat. Mech. (2006) P10004; (2006) P10005.
[45] P. Pfeuty, Ann. Phys. **57**, 79 (1970).
[46] S. Suzuki, J.-i. Inoue, and B. K. Chakrabarti, *Quantum Ising Phases and Transitions in Transverse Ising Models*, Lecture Notes in Physics (Springer, Berlin, 2012).
[47] H. A. Kramers and G. H. Wannier, Phys. Rev. **60**, 252 (1941).
[48] B. Kaufman, Phys. Rev. **76**, 1232 (1949).
[49] M. Ostilli, Europhys. Lett. **97**, 50008 (2012).
[50] S. Brito, A. Canabarro, R. Chaves, and D. Cavalcanti, Phys. Rev. Lett. **124**, 210501 (2020).
[51] H. Nishimori, J. Phys. C: Solid State Phys. **13**, 4071 (1980).
[52] M. Ostilli, J. Stat. Mech. (2007) P09010.